Modulation of Electroenzymatic NADPH Oxidation through Oriented Immobilization of Ferredoxin:$NADP^+$ Reductase onto Modified Gold Electrodes

Juan Madoz-Gúrpide,[†] José M. Abad,[†] Juan Fernández-Recio,[‡] Marisela Vélez,[†] Luis Vázquez,[§] Carlos Gómez-Moreno,[‡] and Victor M. Fernández*,[†]

Contribution from the Departamento de Biocatálisis, Instituto de Catálisis del C.S.I.C., Campus Universidad Autónoma, 28049 Madrid, Spain, Departamento de Fisica e Ingeniería de Superficies, Instituto de Ciencias de Materiales de Madrid del C.S.I.C., Campus Universidad Autónoma, 28049 Madrid, Spain, and Departamento de Bioquímica y Biologia Molecular y Celular, Universidad de Zaragoza, 50006 Zaragoza, Spain

Received April 18, 2000

Abstract: This paper presents a strategy to tune the orientation of immobilized proteins on electrodes of general applicability to different types of proteins. We orient ferredoxin:$NADP^+$ reductase molecules onto a modified gold electrode by introducing a genetically engineered metal binding site on a selected region of the protein surface and covering the gold surface with a self-assembled monolayer of thiols appended with nitrilotriacetic acid groups complexed with metal transition ions. Two mutants were designed to have a histidine pair (His-X_3-His) on surface-exposed α-helices located in one of the two protein domains. It was first demonstrated that the mutant proteins in solution retain their full activity and that the kinetic constants of the redox catalytic steps are not affected by the mutations. The enzyme-modified gold electrodes were then analyzed for the amount and distribution of protein on their surface and for their activity using atomic force microscopy and cyclic voltammetry. The two electrode-bound mutant enzymes manifested differences in the amount and distribution of bound molecules, in the kinetic constants of their redox catalytic steps, and most interestingly, in their ability to transfer electrons to a redox mediator covalently attached to the self-assembled monolayer. We conclude that the position of the mutated α-helix determined the orientation of the protein with respect to the surface and, as a result, its competence to establish direct electrical communication with the electrode.

Introduction

The interest in controlling the orientation and order of macromolecules immobilized on solid surfaces has grown greatly in recent years, the aim of most of the developed strategies being to optimize the interactions between immobilized macromolecules, e.g., nucleic acids, antibodies, or peptides, and their corresponding target molecules in solution as well as with the solid device interface.[1−4] These strategies are also required for the development of biomimetic electrode-coupled supramolecular structures with spatially controlled electron transfer.[5]

Some of the successful general procedures used up-to-date for oriented protein immobilization are based on a modification of the macromolecule by molecular engineering to introduce a specific affinity motif that subsequently binds to a functionalized surface. This approach requires a detailed knowledge of the position of the modification introduced in the protein as well as of the distribution of the binding motifs on the functionalized surface. Site-directed mutagenesis protocols for protein modification[6] and self-assembled monolayers (SAM) for substrate modification[7] meet these requirements, the remaining being the selection of the binding motif that will govern the interaction between the protein and the substrate. Desirable characteristics of these interaction sites are (a) specificity, such that the modified protein binds only through such site to the functionalized substrate, (b) mildness of the modification, such that the protein function is not altered, (c) knowledge and control of the position of the interaction site on the surface of the protein,

* Address correspondence to this author.
[†] Instituto de Catálisis del C.S.I.C.
[§] Instituto de Ciencias de Materiales de Madrid del C.S.I.C.
[‡] Universidad de Zaragoza.

(1) Bambad, C. *Biophys. J.* **1998**, *75*, 1997−2003.
(2) Delamarche, E.; Sundarabaru, G.; Biebuyck, H.; Michel, B.; Gerber, Ch.; Sigrist, H.; Wolf, H.; Ringsdorf, H.; Xanthopoulos, N.; Mathieu, H. J. *Langmuir* **1996**, *12*, 1997−2006.
(3) Kooyman, R. P. H.; van den Heuvel, D. J.; Drijfhout, J. W.; Welling, G. W. *Thin Solid Films* **1994**, *244*, 913−916.
(4) (a) Firestone, M. A.; Shank, M. L.; Sligar, S. G.; Bohn, P. W. *J. Am. Chem. Soc.* **1996**, *118*, 9033−9041. (b) Bourdillon, C.; Demaille, C.; Moiroux, J.; Savéant, J.-M. *Acc. Chem. Res.* **1996**, *29*, 529−535. (c) Sigal, G. B.; Bamdad, C.; Barberis, A.; Strominger, J.; Whitesides, G. M. *Anal. Chem.* **1996**, *68*, 490−497. (d) Katz, E.; Heleg-Shabtai, V.; Willner, B.; Willner, I.; Bückmann, A. F. *Bioelectrochem. Bioenerg.* **1977**, *42*, 95−104. (e) Schmid, E. L.; Keller, T. A.; Dienes, Z.; Vogel, H. *Anal. Chem.* **1997**, *69*, 1979−1985. (f) Ho, C.-H.; Limberis, L.; Caldwell, K. D.; Stewart, R. J. *Langmuir* **1998**, *14*, 3889−3894. (g) Houseman, B. T.; Mrksich, M. *Angew. Chem., Int. Ed.* **1999**, *38*, 782−785. (h) Salamon, Z.; Brown, M.; Tollin, G. *Trends Biochem. Sci.* **1999**, *24*(6), 213-219.
(5) (a) Knoll, W.; Pirwitz, G.; Tamada, K.; Offenhäusser, A.; Hara, M. *J. Electroanal. Chem.* **1997**, *438*, 199−205. (b) Heleg-Shabtai, V.; Katz, E.; Willner, I. *J. Am. Chem. Soc.* **1997**, *119*, 8121−8122. (c) Bardea, A.; Katz, E.; Bückmann, A. F.; Willner, I. *J. Am. Chem. Soc.* **1997**, *119*, 9114−9119.
(6) Smith, M. *Angew. Chem., Int. Ed. Engl.* **1994**, *33*, 1214−1221.
(7) (a) Mrksich, M.; Whitesides, G. M. *Trends Biotechnol.* **1995**, *13*, 228−235. (b) Lairi, J.; Isaacs, L.; Tien, J.; Whitesides, G. M. *Anal. Chem.* **1999**, *71*, 777−790.

10.1021/ja001365m CCC: $19.00
Published on Web 09/23/2000

such that different orientations can be produced at will, and (d) applicability to different types of proteins. Reversibility would be an added value for some applications such as controlled release.

Previous work from this laboratory demonstrated that the chimeric protein produced by the fusion of a choline binding domain from the (acetylmuramoyl)-L-alanine amidase (C-LYTA) from *Streptococcus pneumoniae* and the N-terminal end of the β-galactosidase from *Escherichia coli* binds to a gold substrate where choline had been previously introduced through a step-by-step chemical modification of a thiol based SAM.[8] The binding was shown to be specific and reversible and to leave the hydrolase activity of the galactosidase unaffected. However, the use of such a binding motif restricted the orientation of the protein with respect to the surface to only one position determined by the structure of the chimera protein, since a fusion of the choline binding domain to the C-terminal end of the β-galactosidase resulted in a chimera protein without catalytic activity. In the present work we use a targeting strategy that is also specific and leaves the enzyme activity unaffected, with the additional advantages of allowing different orientations of the same molecule and of being general enough to be applicable to any type of protein. To this aim metal binding sites were genetically engineered on selected regions of a protein surface[9] and offered to self-assembled monolayers terminated on nitrilotriacetic groups complexed with metal transition ions (SAM-TOA-ANTA-Cu^{2+}).

The protein used for these studies is the enzyme ferredoxin: $NADP^+$ reductase (FNR) from the cyanobacterium *Anabaena* PCC 7119.[10] This enzyme catalyzes the reduction of $NADP^+$ to NADPH during photosynthesis by mediating the transfer of two electrons from photosystem I to $NADP^+$ via ferredoxin in two successive one-electron steps.[11] This enzyme was chosen as a model protein in this study for the following reasons: first, oxidoreductases have enzymatic properties which can be exploited for various device applications after incorporation into organized bioassemblies.[12] Second, their incorporation into interfacial architectures on the surface of solid electrodes can be followed by electrochemical techniques.[13] In particular, electron transfer between the prosthetic group and the electrode can be conveniently used to monitor the orientation of the protein molecules with respect to the surface. To this aim FNR is a particularly interesting reductase because the edge of the isoalloxazine ring system, which constitutes the reactive part of the FAD cofactor in electron transfer with ferredoxin, is well exposed to the solvent[10] and therefore could establish electrical contact with properly oriented redox groups anchored onto the monolayer surface. Furthermore, its X-ray structure at 1.8 Å is available[10] and its synthetic genetic machinery has been cloned and expressed in *E. coli*, allowing site-directed mutagenesis.[14,15]

The two mutants designed in this work have a histidine pair (His-X_3-His) in surface-exposed α-helices[16] located in one of the two protein domains (Figure 1). The axis of the helix in the NADPH-binding domain (FNR-II double mutant) is orthogonal to the plane of the isoalloxazine ring of the FAD prosthetic group, whereas the modified helix in the FAD-binding domain (FNR-I single mutant) is parallel to this plane. A predicted consequence of the different location of the binding sites is that upon immobilization on the functionalized SAM, in FNR-II the electron exchanging site of the isoallosazine ring will be facing the electrode whereas in FNR-I it will be directed away from it (Figure 2).

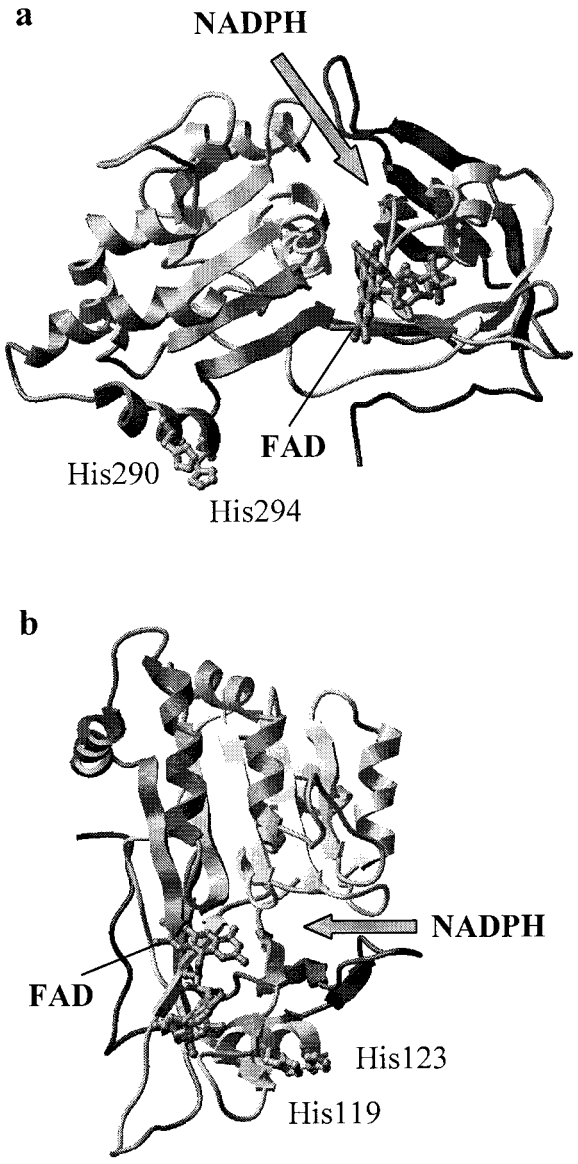

Figure 1. Structural model for the ferredoxin-$NADP^+$ oxidoreductase protein with the engineered metal-binding site: (a) mutant FNR K290H/K294H (these histidine residues are located in a surface-exposed α-helix of the NADPH binding domain) and (b) mutant FNR T119H (the replaced histidine residue and the naturally occurring histidine 123 belong to an α-helix of the FAD binding domain). (Figures were obtained with the ICM program for modeling proteins.[37])

In this work the effect of the mutations on the rate constants of redox reactions catalyzed by the enzymes in solution was investigated through electrochemical analysis. The enzyme-modified gold electrodes were then analyzed for the amount and distribution of the proteins on their surface and for their activity using Atomic Force Microscopy (AFM) and Cyclic

(8) Madoz, J.; Kuznetzov, B. A.; Medrano, F. J.; Garcia, J. L.; Fernández, V. M. *J. Am. Chem. Soc.* **1997**, *119*, 1043−1051.
(9) Zhang, J.-H.; Arnold, F. H. *Trends Biotechnol.* **1994**, *12*, 189−192.
(10) Serre, L.; Vellieux, F. M. D.; Medina, M.; Gómez-Moreno, C.; Fontecilla-Camps, J. C.; Frey, M. *J. Mol. Biol.* **1996**, *263*, 20−39.
(11) Serrano, A.; Rivas, J.; Losada, M. *FEBS Lett.* **1984**, *170*, 85−88.
(12) Nakamura, K.; Aizawa, M.; Miyawaki, O. *Electro-enzymology and coenzyme regeneration*; Springer-Verlag: Berlin, 1988.
(13) Bourdillon, C.; Demaille, C.; Moiroux, J.; Savéant, J.-M. *J. Am. Chem. Soc.* **1993**, *115*, 12264−12269.
(14) Fillat, M. F.; Bakker, H. A. C.; Weisbeek, P. J. *Nucleic Acids Res.* **1990**, *18*, 7161.
(15) Gómez-Moreno, C.; Martinez-Júlvez, M.; Fillat, M. F.; Hurley, J.; Tollin, G. *Photosynthesis: from Light to Biosphere*; Mathis, P., Ed.; Kluwer Academic Publishers: Dordrecht, The Netherlands, 1995; Vol. II, pp 627−632.
(16) Arnold, F. H.; Haymore, B. L. *Science* **1991**, *252*, 1796−1797.

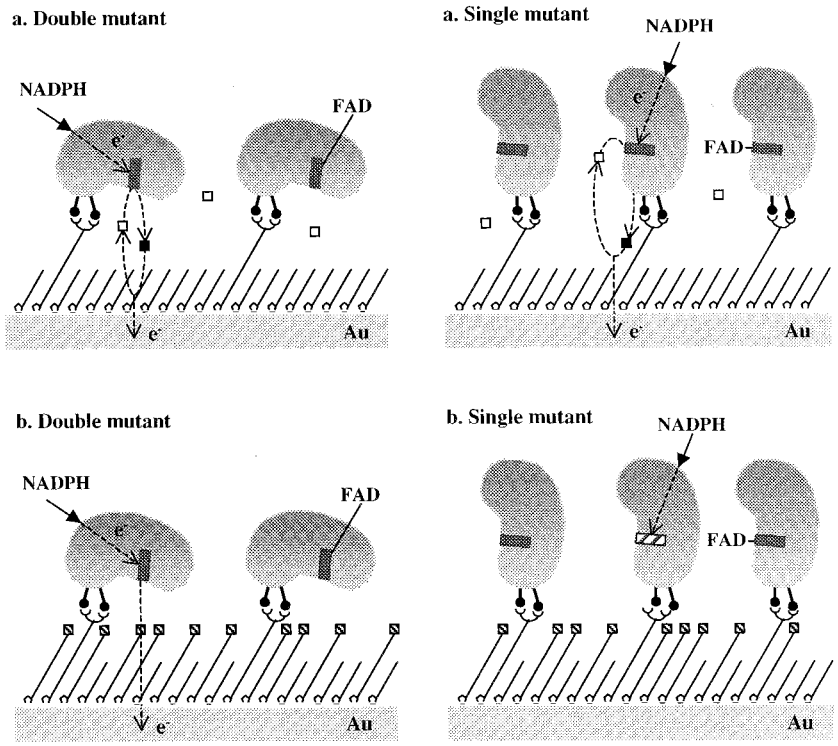

Figure 2. Schematic depiction of FNR engineered mutants (double and single) immobilized through the interaction of a His-X_3-His motif (•) with Cu^{2+} chelated to a SAM-TOA-ANTA. Electrons from NADPH can be fed to the gold electrode either through soluble redox mediators (□ oxidized, ■ reduced) (a) or through covalently attached ones (⧅) (b).

Voltammetry (CV). Mixed SAMs of nitrilotriacetic-Cu^{2+} and ferrocene were used to investigate how the orientation of the enzyme on the SAM modulates the wiring of its active site to redox groups on the monolayer.

Experimental Section

Gold-Supports Preparation. Polycrystalline gold wire electrodes were polished and cleaned and their effective areas (typically 0.3 cm^2) determined from chronocoulometric Anson plots with ferricyanide as previously described.[8] Glass supports (1.1 × 1.1 cm) covered with evaporated gold layers (0.2−0.3 μm) deposited over a chromium adhesion layer (1−4 nm) (Metallhandel Schröer GmbH) were used for AFM; they were cleaned with piranha solution following the method and warnings described by Bain et al.,[17] followed by 2 min of annealing in a gas flame. After the cleaning treatment, the gold surfaces were covered with a monolayer of dithioctic acid (TOA; Sigma) and subjected immediately to carboxylic activation with *N*-hydroxysuccinimide (NHS; Sigma) as described.[8]

Synthesis of 1-[*N*-(methylferrocenyl)amino]-8-amino-3,6-dioxaoctane. This molecule (DADOOFc) was synthesized with a variation of the method described by Schuhmann et al.[18] Ferrocenecarboxaldehyde (250 mg; Sigma) dissolved in 20 mL of methanol was added to a solution of 1,8-diamino-3,6-dioxaoctane (DADOO; Merck) (0.68 mL) in 30 mL of anhydrous methanol and 4 Å molecular sieve, at room temperature. Then, an excess of sodium borohydride (146 mg) in water was dropped into the solution, and the reaction mixture was stirred overnight. The solvent mixture was rotavaporated to dryness and the residue was dissolved in water, pH adjusted to 10 with potassium carbonate, extracted with ethyl ether, dried with anhydrous sodium sulfate, filtered, concentrated, and eluted through a silica gel column employing trichloromethane as mobile phase. Yield 68%. ^{1}H NMR (250 MHz) δ 1.8 pm (s, 3H), 2.77 (t, 4H), 3.42 (m, 4H), 3.52 (m, 6H), 4.03 (t, 2H), 4.07 (s, 5H), 4.13 ppm (t, 2H); *m*/*z*: 346 (M^+ 44), 199 (100). Anal. ($C_{17}H_{26}N_2O_2Fe$) Calcd: C, 58.95; H, 7.51; N, 8.09. Found: C, 58.92; H, 7.58; N, 8.09.

Synthesis of *N*-(5-Amino-1-carboxypentyl)iminodiacetic Acid (ANTA). The compound H_2N-$(CH_2)_4$-CH(COOH)N$(CH_2COOH)_2$ was synthesized from N^6-benzyloxycarbonyl-L-lysine (Sigma) as described by Hochuli et al.[19] The product was stored under nitrogen. ^{1}NMR spectrum (D_2O) 1.22−1.79 (6H, m), 2.64 (2H, t; J = 6.70 Hz), 3.05 (4H, d; J = 3.81 Hz), 3.28−3.33 ppm (1H, m); *m*/*z* 262 (M^+). Anal. ($C_{10}H_{18}N_2O_6$) Calcd: C, 52.17; H, 7.83; N, 12.17; O, 27.83. Found: C, 51.9; H, 7.5; N, 12.3; O, 28.3.

Synthesis of SAM-TOA modified with Nitrilotriacetic-Cu^{2+}. Amidation of NHS-esters of SAM-TOA was effected overnight in a 0.15 M solution of ANTA in DMF/H_2O (2:1), followed by DMF washing (SAM-TOA-ANTA). Alternatively, mixtures of ANTA and ethanolamine (EA; Aldrich) were used to prepare electrodes in which the ANTA ligands were diluted with shorter hydroxy-ending molecules (SAM-TOA-[ANTA-EA]). The last step consisted of dipping the modified electrode in a 40 mM $CuSO_4$ water solution at pH 5.5 (acetate buffer 50 mM) for 1 h. All electrode preparations were run in duplicate. All solutions were prepared with Millipore (Milli-Q plus) water (18.2 MΩ cm).

Synthesis of SAM-TOA-[ANTA-DADOOFc]. In a similar way, mixtures of ANTA and DADOOFc were used to prepare electrodes in which the redox mediator was covalently bound to the SAM-TOA.

Detection of SAMs. Control electrodes were used for SAM evaluation with cyclic voltammetry in 0.5 M KOH in the potential range 0 to −1.1 V. The presence of a reductive wave at −1.0 V was taken as evidence for the existence of a thiol SAM. From the peak charge the surface coverage by sulfur atoms was estimated, assuming a value of one electron per sulfur atom.[20]

Preparation and Characterization of the FNR Mutants. Single (T119H, FNR-I) and double (K290H/K294H, FNR-II) mutants of the enzyme ferredoxin:$NADP^+$ reductase from *Anabaena* PCC 7119 were

(17) Bain, C. D.; Evall, J.; Whitesides, G. M. *J. Am. Chem. Soc.* **1989**, *111*, 7155−7164.
(18) Schuhmann, W.; Ohara, T. J.; Schmidt, H.-L.; Heller, A. *J. Am. Chem. Soc.* **1991**, *113*, 1394−1397.
(19) Hochuli, E.; Döbeli, H.; Schacher, A. *J. Chromatogr.* **1987**, *411*, 177−184.
(20) Walczak, M. M.; Popenoe, D. D.; Deinhammer, R. S.; Lamp, B. D.; Chung, C.; Porter, M. C. *Langmuir* **1991**, *7*, 2687−2693.

generated by introducing mutations in the gene of the enzyme FNR[14] by site-directed mutagenesis using the method described by Deng and Nickoloff.[21] Mutations did not alter chromatographic properties during FNR purification, so mutant proteins were purified in essentially the same way as recombinant wild-type FNR.[15] Kinetic and spectral properties of mutant proteins indicated no major structural modification with respect to the native protein.

The ability of mutant proteins to bind metal ions was determined by immobilized metal ion affinity chromatography (IMAC),[22] using iminodiacetic acid (IDA)-agarose[23] pre-packed columns from Sigma. The columns were filled with Cu^{2+} or Ni^{2+} ions by loading five volumes of 20 mM $CuSO_4$ or $Ni(NO_3)_2$ solutions, respectively. Columns were equilibrated with 20 mM sodium phosphate, 1 M NaCl, pH 7. Purified proteins were dialyzed against the standard buffer (20 mM sodium phosphate, 1 M NaCl, pH 7) prior to being poured into the columns. Weakly bound proteins were eluted by a pH change with 20 mM sodium acetate, 1 M NaCl, pH 5.5, while strongly bound proteins were eluted with 30 mM imidazole in 20 mM sodium phosphate, 1 M NaCl, pH 7. All chromatography experiments were performed at 4 °C. Mutants K290H/K294H and T119H strongly bound Cu^{2+}-IDA-agarose columns. Mutant II strongly bound to Ni^{2+} columns while mutant I binding was weaker, suggesting that metal ion binding sites introduced in mutant II is stronger than the one formed in mutant I. This is in agreement with previous reports that the metal binding affinity toward imidazol follows the order Cu(II) > Ni(II) > Zn(II) > Co(II).[23c] Wild-type FNR was retained neither in Cu^{2+} nor in Ni^{2+} columns.

Enzymatic Assays and Protein Measurements. The diaphorase activity of soluble FNR (wild-type enzyme and mutants) was assayed spectrophotometrically at 25 °C with 0.035 mM 2,6-dichlorophenol-indophenol (DCPIP; Sigma) as electron acceptor and 0.12 mM NADPH (Sigma) as electron donor in 50 mM phosphate buffer, pH 7.5.[24] This assay was also used to estimate the amount of protein immobilized on the electrodes after desorption of the protein with 100 mM imidazole in 50 mM phosphate buffer, pH 7.5, followed by 2.5 times dilution with imidazole-free buffer containing 0.25 mM NADPH, 0.058 mM DCPIP. Control experiments showed that 40 mM imidazole did not inhibit FNR activity under the assay conditions. Diaphorase activity was also assayed electrochemically with ferrocenemethanol.[25] Antibodies raised against FNR were used for independent measurements of electrode-immobilized protein in a conventional ELISA immunocompetition assay.[26]

Apparatus. Cyclic voltammetry and X-ray Photoelectron Spectroscopy (XPS) data were obtained as previously described.[8] Electrochemical meaurements were carried out using an Ag/AgCl, 3 M NaCl, reference electrode. All potentials are reported with respect to this reference electrode. Copper content in solutions was determined with an Atomic Emission Inductively Coupled Plasma (AES-ICP) spectrophotometer, Optima 3300 DV (Perkin-Elmer). AFM was carried out with a Nanoscope III Microscope (Digital Instruments) in the tapping mode in solution.

Results

Electrochemical Analysis of the Two Mutant Proteins in Solution. The FNR has, besides the genuine ferredoxin-$NADP^+$ oxidoreductase activity, the capability of catalyzing the oxidation of NADPH with artificial electron acceptors (diaphorase activity).[24] Our previous work showed that FNR also catalyzes the oxidation of NADPH with the oxidized form of ferrocenemethanol (FM_{ox})[25] according to the following sequence of reactions:

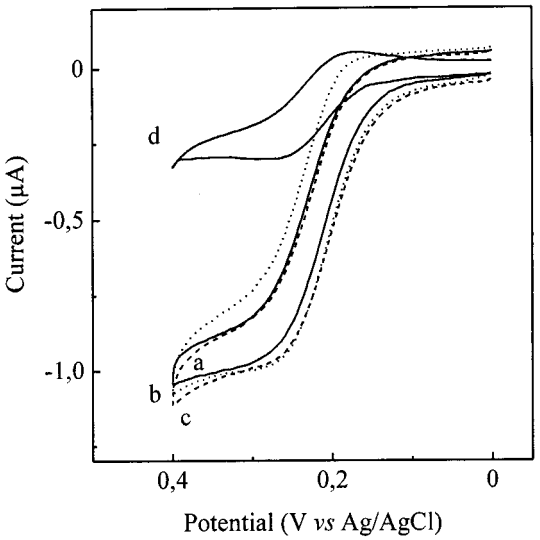

Figure 3. Cyclic voltammograms of 20 μM ferrocenemethanol on a gold electrode, before and after the addition of 2 mM NADPH, in the presence of catalytic amounts (10^{-7} M) of (a, solid line) FNR−II mutant, (b, dotted line) FNR wild type, (c, dashed line) FNR-I mutant, and (d, solid line) FNR-II in the absence of substrate. Scan rate 10 mV s^{-1}. Conditions: 50 mM phosphate buffer plus 0.15 M KCl, pH 7.5.

$$\mathrm{FNR} + \mathrm{NADPH} \underset{k_{-1}}{\overset{k_1}{\rightleftharpoons}} \mathrm{FNR{-}NADPH} \qquad (1)$$

$$\mathrm{FNR{-}NADPH} + \mathrm{H^+} \xrightarrow{k_2} \mathrm{FNRH_2} + \mathrm{NADP^+} \qquad (2)$$

$$\mathrm{FNRH_2} + 2\mathrm{FM_{ox}} \xrightarrow{k_3} \mathrm{FNR} + 2\mathrm{FM_{red}} + 2\mathrm{H^+} \qquad (3)$$

The first step consists of the reversible binding of the enzyme to the NADPH substrate forming the transient complex FNR−NADPH (eq 1), which allows the transfer of the hydride to the FAD (eq 2). Then, the reduced enzyme transfers the electrons to the FM_{ox} generated at the surface of the electrode during the anodic scan in a cyclic voltammogram, two FM_{ox} molecules being required to regenerate the initial oxidized form of FNR. The electrochemical responses of ferrocenemethanol on a gold electrode, before and after the addition of NADPH, in the presence of catalytic amounts of the double mutant are shown in Figure 3a. The increase of the anodic current until reaching a plateau and the disappearance of the reduction peak on the voltammogram of ferrocenemethanol after the addition of NADPH are the two most noticeable features. The cathodic scan almost retraces the anodic one, indicating, first, that the catalytic reduction of FM_{ox} is faster than the diffusion of ferrocenemethanol to the electrode and, second, that the consumption of NADPH within the diffusion layer is negligible. Comparable CVs are obtained with the wild-type[25] and the single mutant (Figure 3, traces b and c, respectively).

The kinetic constants of the two mutants in solution, at pH 7.5, were extracted from cyclic voltammograms with different concentrations of substrates, according to the methodology described by Bourdillon et al.[27] The ferrocenemethanol concentration ranged from 1.25×10^{-6} to 10^{-4} M and that of

(21) Deng, W. P.; Nickoloff, J. A. *Anal. Biochem.* **1992**, *200*, 81−88.
(22) Porath, J.; Carlsson, J.; Olsson, J.; Belfrage, G. *Nature* **1975**, *258*, 598−599.
(23) (a) Porath, J.; Olin, B. *Biochemistry* **1983**, *22*, 1621−1630. (b) Todd, R.; Van Dam, M. E.; Casimiro, D.; Haymore, B. L.; Arnold, F. H. *Proteins* **1991**, *10*, 156−161. (c) Sundberg, R. J.; Martin, R. B. *Chem. Rev.* **1974**, *74*, 471−517.
(24) Koike, M.; Hayakawa, T. *Methods Enzymol.* **1970**, *18*, 298−307.
(25) Madoz, J.; Fernández-Recio, J.; Gómez-Moreno, C.; Fernández, V. M. *Bioelectrochem. Bioenerg.* **1998**, *47*, 179−183.
(26) (a) Engvall, E. *Methods Enzymol.* **1980**, *70*, 419−439. (b) O'Kennedy, R.; Byrne, M.; O'Fagain, C.; Berns, *G. Biochem. Educ.* **1990,** *18*, 136−140.
(27) Bourdillon, C.; Demaille, C.; Gueris, J.; Moiroux, J.; Savéant, J.-M. *J. Am. Chem. Soc.* **1993**, *115*, 12264−12269.

Table 1. Calculated Rate Constants for NADPH Oxidation

enzyme	k_3 (M^{-1} s^{-1})	k_2 (s^{-1})	k_{red} (M^{-1} s^{-1})
	in solution		
native FNR	$(7.0 \pm 1.4) \times 10^5$	430 ± 90	$(1.5 \pm 0.7) \times 10^4$
FNR K290H/K294H	$(6.2 \pm 1.5) \times 10^5$	410 ± 70	$(1.8 \pm 0.4) \times 10^4$
FNR T119H	$(6.2 \pm 0.4) \times 10^5$	400 ± 160	$(1.7 \pm 0.3) \times 10^4$
	electrode		
FNR K290H/K294H	$(6.8 \pm 0.5) \times 10^5$	420 ± 60	$(1.9 \pm 0.6) \times 10^4$
FNR T119H	$(4.8 \pm 0.9) \times 10^5$	240 ± 100	$(0.9 \pm 0.4) \times 10^4$

[a] $n = 8$ measurements for every set of experiments.

NADPH from 5×10^{-4} to 5×10^{-3} M. The enzyme concentration was maintained constant throughout all experiments at 10^{-7} M. The values of rate constants, k_2, k_3, and $k_{red} = k_1k_2/(k_{-1} + k_2)$ calculated for the wild-type enzyme and for the two mutants are given in Table 1.[28] It can be observed that the introduction of the histidine pairs in these two different α-helices of native FNR does not change the catalytic parameters of the soluble form of the enzyme.

Stepwise Construction of the Nitrilotriacetic-Functionalized SAM. The starting monolayer used in these studies is a TOA-SAM with an estimated surface coverage near the monolayer, $(7.5 \pm 0.6) \times 10^{-10}$ mol cm^{-2}, that has been shown to have the required stability and permeability to electrochemical probes.[8] The carboxy terminal groups in the monolayer were activated by esterification with *N*-hydroxysuccinimide in dioxane, to facilitate the covalent link of ANTA through the free amine groups. The reductive desorption wave of the monolayer modified with nitrilotriacetic acid had a charge that corresponds to a thiolate surface coverage of $(7.2 \pm 0.6) \times 10^{-10}$ mol cm^{-2} ($n = 5$), which implies that the further modification of the TOA monolayer did not significantly affect the gold thiol coverage.

In the present work we have used two differently charged electrochemical probes to ascertain the incorporation of Cu(II) to the NTA groups on the SAM-TOA-ANTA. The response of the electrode to different electrochemical probes provides information on the degree of ionization of the exposed functional groups of the monolayer. At pH 5.5 a full suppression of the response to ferricyanide of TOA covered electrodes was observed (see Supporting Information, Figure Sla), and also with SAM-TOA-ANTA coverage (Figure Slb). Soaking the SAM-TOA-ANTA electrode during 1 h in a 40 mM $CuSO_4$ water solution at pH 5.5 partially restored the response to ferricyanide (Figure Slc) which is indicative of a neutralization of carboxylates by metal chelation.

The presence of Cu^{2+} in the monolayers was confirmed by XPS and was quantified by atomic emission spectroscopy (AES-ICP). XPS analysis of the SAM-TOA-ANTA-Cu^{2+} monolayer indicated the presence of S, C, N, O, and Cu, besides Au (Table 2). No other element was detected. The atomic ratios found were 0.46 for Cu/N and 0.85 for S/N. The amount of Cu^{2+} ions bound to the monolayer was also estimated by AES-ICP after reductive desorption of the monolayer in alkali (10 min at −1.2 V vs Ag/AgCl in 0.5 M KOH), and was 2.8×10^{-10} mol cm^{-2}. The copper recovered from the electrode indicates that more than 80% of the dithioctic chains have been complexed to Cu^{2+}. Taken together, the results described above support the structure proposed for the SAM-TOA-ANTA-Cu^{2+} in Figure 4.

Enzyme-Modified Electrode. Evidence of the binding of the mutant proteins to the electrode was obtained by analysis of their diaphorase activity with NADPH as electron donor and ferricinum methanol as electron acceptor. Figure 5 shows a cyclic voltammogram of ferrocenemethanol using SAM-TOA-ANTA-Cu^{2+} gold electrodes which, prior to insertion in the electrochemical cell, were incubated in 50 mM phosphate buffer solutions containing 5 mM imidazole and respectively 1.4 μM of (a) wild-type FNR, (b) FNR-II mutant, and (c) FNR-I mutant. Only the electrodes incubated in the presence of the genetically modified proteins gave an electrochemical response in the presence of the substrate NADPH.

The activity of the electrode-bound enzyme was also measured spectrophotometrically monitoring the color changes accompanying DCPIP reduction with NADPH as electron donor.[29] Electrodes incubated in the presence of mutated enzyme and introduced in a cuvette with magnetic stirring produced a decrease in the absorption at 600 nm, whereas the electrode previously incubated in the presence of the wild-type protein did not produce any changes in the absorption at this wavelength (data not shown).

The amount of enzyme bound to the electrode surface was calculated from activity measurements after desorption with 100 mM imidazole. The solubilized protein was also measured by an ELISA assay and the measurements gave consistent values with the amount of protein inferred from enzymatic activity (Table 3).

Dependence of the Protein Binding on the Composition of the Monolayer. In their work on the optimization of biotin-functionalized monolayers for avidin adsorption, Spinke et al.[27] found that the best results were obtained by dilution of the biotinylated chain with shorter hydroxythiols. Consequently, ANTA was diluted with variable amounts of EA for the coupling reaction with the activated carboxylic SAM. We have used different dilutions of ANTA with EA, at the second step of monolayer construction, to study the influence of this dilution effect on the FNR mutants binding. If we assume a similar reactivity of EA and ANTA toward hydroxysuccinimide esters of thiocarboxylic monolayer, then the molar fraction of nitrilotriacetic in the monolayer (X_B) corresponds to the molar fraction of ANTA present in the reaction with succinimide esters. Dilution of ANTA with the shorter hydrophilic chain, EA, produces a large increase of the bound protein reaching a plateau at $X_B = 0.2$ (Table 4). Spinke et al.[29] observed a similar effect of surface-biotin dilution on the adsorption of streptavidin molecules and explained it as being due to steric hindrance in the undiluted biotin layer. A similar explanation could apply to our case. The larger value of X_B at which maximum protein adsorption is observed would be due to the lower size of the FNR molecules as compared with streptavidin.

Binding Specificity. To confirm that the binding was due to the formation of a complex between the chelate and the two histidines introduced in the protein, the electrodes were incubated in the presence of 100 mM imidazole for 30 min (Figure 6b). This analogue of the histidine residue was capable of reversibly displacing the proteins from the electrode surface. Other proofs of the specificity of the binding domain were that the absence of Cu^{2+} in the monolayer prevented the binding of the mutant proteins to the electrode (Figure 6c), and that addition of 100 mM ethylenediaminetetraacetic acid (EDTA) for 30 min prompted the desorption of the protein, as indicated by CV experiments (Figure 7b).

Electrochemical Characterization of the Two Enzymatic Electrodes. The kinetic constants of the single and double

(28) Slightly higher values of k_3 and k_2 previously reported in ref 25 for the wild-type FNR were obtained with a different batch of enzyme. The experiments reported in the present work were done with samples of wild-type and mutant enzymes prepared at the same time and stored under similar conditions.

(29) Spinke, J.; Liley, M.; Schmitt, F. J.; Guder, H. J.; Angermaier, L.; Knoll, W. *J. Chem. Phys.* **1993,** *99,* 7012−7019.

Table 2. XPS Analysis of the SAM-TOA-ANTA-Cu^{2+} Monolayer Indicated the Presence of S, C, N, O, and Cu, besides Au[a]

SAM structure	$Au4f_{7/2}$	C1s	N1s	O1s	S2p	$Cu2p_{3/2}$	Cu/N	S/N
SAM- TOA-ANTA		284.9[2]		531.8[6]				
	83.8[1]		400.1[5]		161.8[8]			
		286.5[3]		533.0[7]				
		288.1[4]						
SAM-TOA-ANTA-Cu^{2+}		284.9		531.5[6]				
	83.8[1]		400.3[5]		162.1[8]	934.4[9]	0.46	0.48
		286.5[3]		532.3[7]				
		288.4[4]						

[a] The atomic ratios found, 0.46 for Cu/N and 0.85 for S/N, were consistent with the proposed structure of the monolayer in Figure 4. The assigned atomic species were the following (designated by superscript numbers 1−9): (1) Au; (2) C−C; (3) C−N; (4) C═O; (5) −CN; (6) C−OH; (7) C═O; (8) S^{2-}; (9) Cu^{2+}.

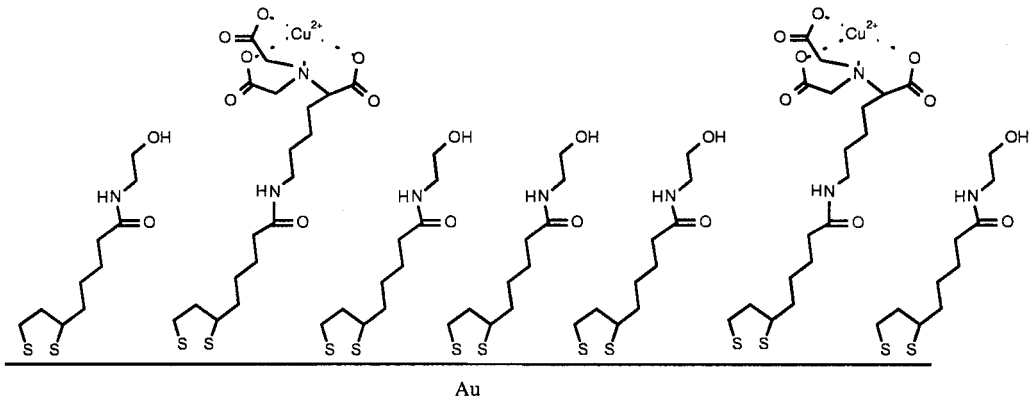

Figure 4. Proposed structure of a monolayer containing TOA-[ANTA:EA]-Cu^{2+} chains. Alternatively, mixtures of ANTA and aminoferrocene were used to prepare electrodes in which the redox mediator was covalently bound to the SAM-TOA.

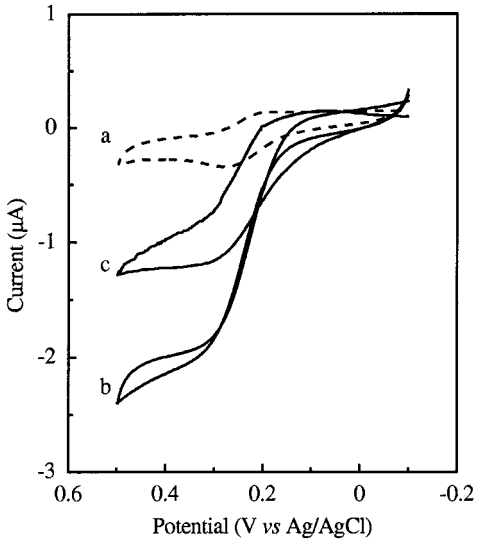

Figure 5. Cyclic voltammogram of ferrocenemethanol using SAM-TOA-ANTA-Cu^{2+} gold electrodes which, prior to insertion in the electrochemical cell, were incubated in 50 mM phosphate buffer solutions containing 5 mM imidazole and 1.4 μM of (a) native FNR, (b) FNR-II mutant, and (c) FNR-I mutant. Other conditions were as in Figure 3.

mutants immobilized on SAM-TOA-ANTA-Cu^{2+} gold electrodes were also measured by cyclic voltammetry, according to the method developed by Bourdillon et al.[13] Previous to the characterization of the system, it is necessary to check that the binding of the enzyme does not affect the reversibility of the mediator on the SAM-modified electrode. In the absence of the NADPH substrate, at pH 7.5 (0.15 M ionic strength), the mediator FM gives rise to a one-electron (chemically and electrochemically) reversible cyclic voltammetric wave (not shown). The anodic peak current remains proportional to the square root of the scan rate up to 10 V s^{-1}; the anodic-to-cathodic peak potential separation remains equal to 60 mV up to 1 V s^{-1}, and both peaks have similar currents. The heterogeneous electron-transfer rate constants (k_o) for ferrocenemethanol measured with SAM-TOA-ANTA-Cu^{2+} electrodes after incubation in solutions of FNR-I or FNR-II were respectively 0.04 ± 0.01 ($n = 6$) and 0.05 ± 0.01($n = 6$) cm s^{-1}.

Table 3. Calculated Amount of the Coverage of the Two Protein Mutants Per Unit Geometric Area of the Modified Electrodes

enzyme	Γ_E (mol × cm^{-2})	n
FNR K290H/K294H	$(4.4 \pm 0.7) \times 10^{-12}$	10
FNR T119H	$(7.6 \pm 1.5) \times 10^{-12}$	10

Table 4. Estimated Amount of Protein Bound to the Modified Electrode as a Function of the Mole Fraction of ANTA in the Monolayer Synthesis, Obtained from a FNR Diaphorase Activity Assay (see Experimental Section)[a]

X_B	amount of protein (ng)	$\Gamma_E^0 \times 10^{12}$ (mol cm^{-2})
1	132 ± 12	4.6 ± 0.4
0.2	144 ± 15	5.0 ± 0.5
0.11	109 ± 12	3.8 ± 0.4
0.03	26.3 ± 3.5	0.9 ± 0.1
0.01	5.3 ± 0.3	0.2 ± 0.0
0 (control)	0	0

[a] Note that XB does not necessarily represent the mole fraction of nitroltriacetic groups in the monolayer.

For the electrocatalytic activity measurements of the FNR electrodes, ferrocenemethanol concentration was fixed at 10 μM (there is no need in this method to vary the mediator concentration[13]) and that of NADPH ranged from 2.5×10^{-4} to 5×10^{-3} M. The maximum value of Γ_E^0 (total amount of enzyme present on the electrode surface) was determined to be $(1.1 \pm 0.5) \times 10^{-12}$ mol with the 0.5 mm diameter gold wire electrodes

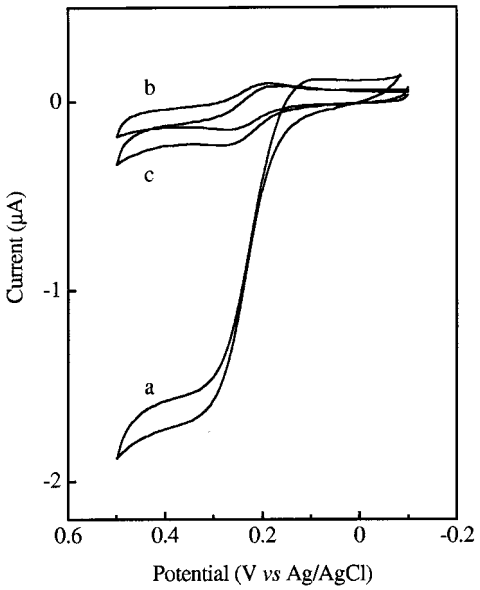

Figure 6. Cyclic voltammetry measurements of the enzymatic activity of SAM-TOA-ANTA-Cu^{2+} electrodes incubated in (a) a 1.4 μM solution of FNR-II mutant (control experiment), (b) a solution of FNR-II mutant but in the presence of 100 mM imidazole, and (c) a solution of FNR-II mutant in the absence of Cu^{2+} in the monolayer. Other experimental conditions were as in Figure 3.

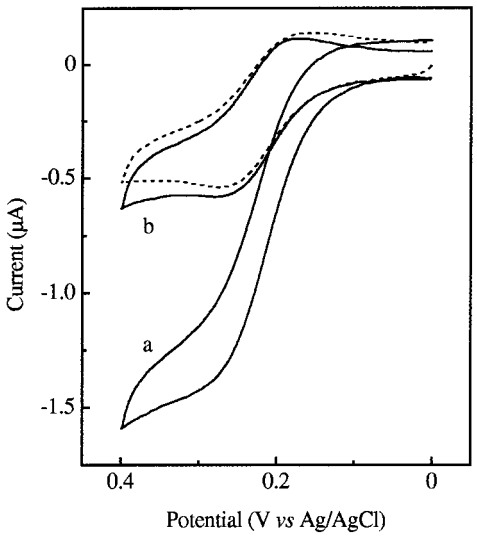

Figure 7. Cyclic voltammogram of 20 μM ferrocenemethanol in the presence of 2.5 mM NADPH measured with a SAM-TOA-ANTA-Cu^{2+} electrode incubated in mutant FNR-II solution (a) and 30 min after the addition of 100 mM EDTA (b). Dashed lines give the CV in the absence of NADPH. Other experimental conditions were as in Figure 3.

we used for the CV experiments, that is, $(4.4 \pm 0.7) \times 10^{-12}$ mol cm^{-2} (Table 3) per unit geometric area. Figure 8 shows typical voltammograms of the catalytic reactions ocurring when NADPH is added into the bulk solutions where the enzymatic electrodes are placed. We checked that the magnitude of i_{cat} was independent of the scan rate, as predicted by Bourdillon et al.[13] The values of rate constants k_2, k_3, and k_{red} for the two enzymatic electrodes are also given in Table 1. Figures S2 and S3 (see Supporting Information) show examples of the plots used to calculate these constants for a series of experiments.

Orientation of the FNR Molecules on the Electrode Surface. As an indication of a different orientation of FNR molecules, dependent on the binding motif position, we

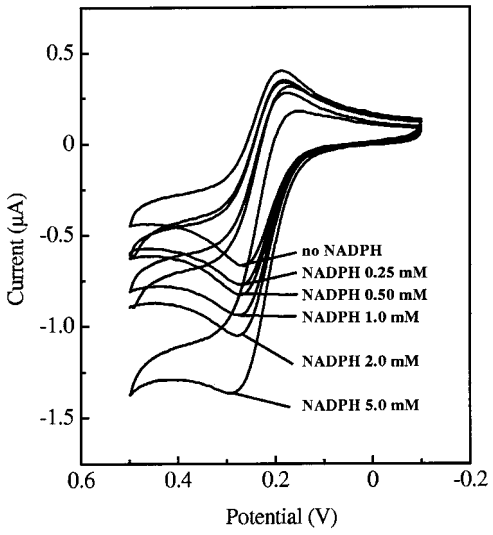

Figure 8. Cyclic voltammograms of 20 μM ferrocenemethanol obtained with a SAM-TOA-[ANTA-EA, 1:4]-Cu^{2+} modified electrode, run in different NADPH concentrations (from 0 to 5×10^{-3} M). Other experimental conditions were as in Figure 3.

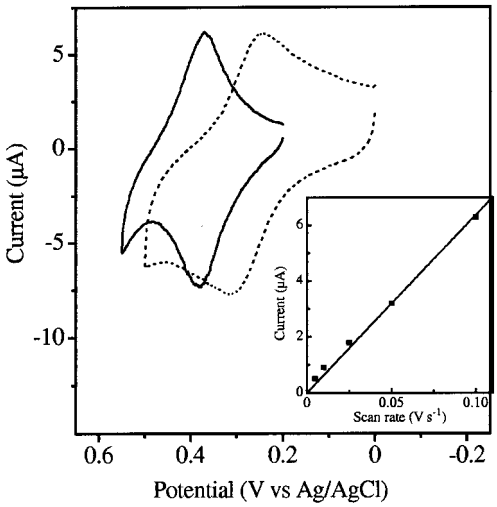

Figure 9. Cyclic voltammogram in 50 mM phosphate buffer (pH 7.5, 0.1 M KCl) of gold electrode covered with SAM-TOA-DADOOFc (solid line). The dashed line gives a CV of DADOOFc in solution (10^{-4} M). The scan rate was 0.1 V s^{-1}. The inset shows the linear correlation between the peak current and the scan rate of immobilized DADOOFc.

investigated the electrocatalytic NADPH oxidation mediated by ferrocene covalently bound in a mixed SAM-TOA-[ANTA-DADOOFc, 1:10].

First of all, we investigated the electrochemical behavior of a SAM-TOA-DADOOFc (Figure 9, solid line). The nearly symmetric CV is suggestive of species immobilized on a monolayer.[30] The peak current densities, j_a and j_c, had the same value and increased linearly with the scan rate (inset of Figure 9). A surface concentration of 2.5×10^{-10} mol cm^{-2} for the immobilized ferrocene was determined from the charge of the CV peaks, assuming a one-electron reduction. This coverage agrees quite well with that reported by Rowe and Creager[31] for SAMs of the single thiol Fc-C_6-SH. The redox potential of the one-electron oxidation of immobilized ferrocene ($E° = 375$ mV) was significantly more positive than the oxidation potential of ferrocene in solution ($E° = 278$ mV) (Figure 9), in agreement with previous reports.[8,31] ΔE_p observed was 10 mV and the

(30) Abruña, H. D. *Coord. Chem. Rev.* **1988**, *86*, 135−189.
(31) Rowe, G. K.; Creager, S. E. *Langmuir* **1994**, *10*, 1186−1192.

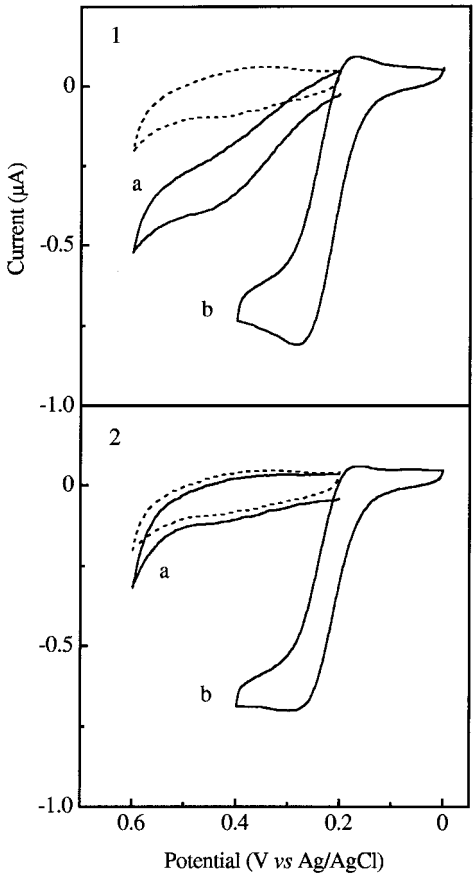

Figure 10. Electrochemical behavior of electrodes of SAM-TOA-[ANTA-DADOOFc, 1:10]-Cu^{2+}. (la) CV of the electrode incubated with FNR-II mutant in the presence of 1 mM NADPH without soluble mediator. (lb) As above, recorded after the addition of ferrocenemethanol, final concentration 50 μM. (2a) CV of an electrode incubated with FNR-I mutant in the absence of soluble redox mediator, NADPH 1 mM. (2b) CV of the same electrode after addition of ferrocenemethanol, 50 μM. Dashed lines show the cyclic voltammograms of the SAM-TOA-[ANTA-DADOOFc, 1:10]-Cu^{2+} electrodes prior to NADPH addition. Scan rate 10 mV s^{-1}. The supporting electrolyte was 50 mM phosphate buffer with 50 mM $NaClO_4$, pH 7.

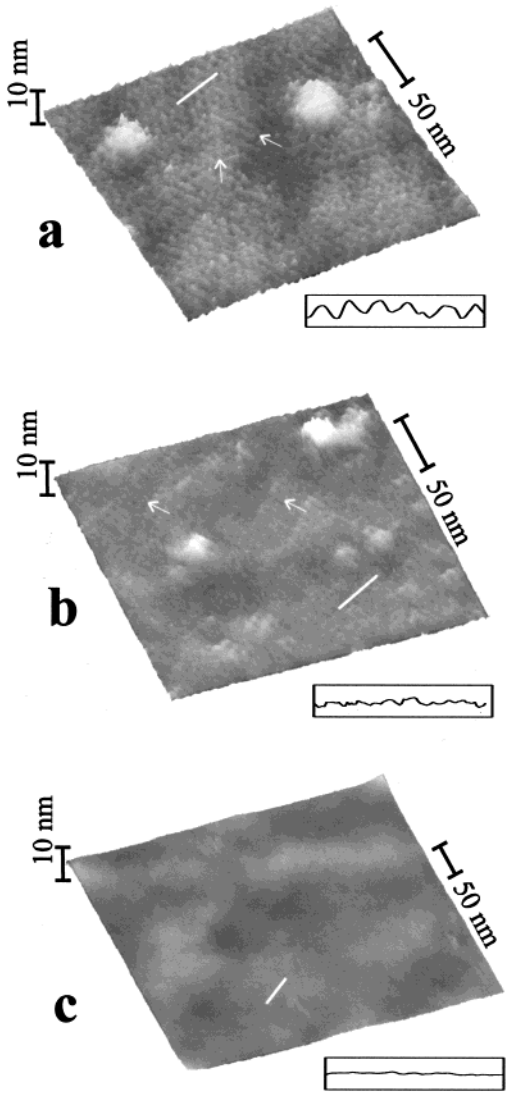

Figure 11. Surface topography of a SAM-TOA-ANTA-Cu^{2+} modified electrode: (a) incubated with FNR-II protein; (b) incubated with FNR-I protein; and (c) incubated in buffer solution. The white arrows indicate the direction of protein alignment. The insets show the height profile of the white lines indicated in the pictures. In all three cases the height and length of the insets are 2 and 50 nm, respectively.

width of the peak at half-height was 94 mV, close to the theoretical value of 90.6/*n* mV ($n = 1$) expected for an ideally reversible process of immobilized species on a monolayer.

Electrodes covered with SAM-TOA-[ANTA:DADOOFc, 1:10]-Cu^{2+} were incubated with FNR-I or FNR-II mutants and analyzed for catalytic activity after NADPH addition (Figure 10). The electrode with mutant FNR-II showed catalytic activity in the presence of NADPH, whereas the electrode with FNR-I only showed catalytic activity after addition of NADPH plus soluble ferrocenemethanol. These results indicate that the FNR-I enzyme on the electrode, although catalytically active, was unable to establish electrical communication with the gold substrate. On the contrary, the mutant FNR-II was wired to the gold substrate through ferrocene molecules in the monolayer.

Structural Characterization of the FNR Electrodes. Analysis of the surface of the modified electrode with scanning force microscopy provided information about the coverage and disposition of the enzyme molecules on the electrode surface. After incubation with a solution of mutant FNR-II, the surface is fully covered by an ordered array of proteins (Figure 11a). The width of the protein rows corresponds to the expected 5 nm width[10] of the individual protein molecules oriented with their long axis parallel to the substrate. Considering that the separation of the rows is 10 nm, the percentage of electrode surface covered by protein measured directly from the images is 60%, which corresponds quite well with the expected covered area calculated from the surface projection of the amount of protein measured using other techniques (Table 3). The surface of the electrode incubated in mutant FNR-I (Figure 11b) presented a different structure, since although also fully covered with a protein layer, the individual protein molecules were more closely packed and presented short range order only. The distance between the protein rows was 4−6 nm, which is close to the width of the individual protein molecules. The low contrast of the images is therefore due to the tightness of the protein array, which does not allow the microscope tip to penetrate between rows. This denser appearance of the protein monolayer is in accordance with the other experimental results that show that this mutant yields 1.7 times more protein per unit electrode area than the mutant FNR-II. At least three electrodes with each of the mutants were analyzed with different microscope tips, and the described difference in protein arrangement was observed in all of them. For the sake of

comparison, Figure 11c shows the appearance of the gold surface modified with SAM-TOA-ANTA-Cu^{2+}.

Discussion

The increasing number of available crystallographic structures of proteins is a source of inspiration for the design of proteins with novel functions. For example, the knowledge that metal ions play important roles in the function and stability of protein structures has prompted the synthesis ex novo by site-directed mutagenesis of metal binding sites, either to mimic the geometry and catalytic features of natural sites or to endow the proteins with new specific properties.[32] Several studies by Arnold have evidenced the usefulness of this approach for the stabilization or purification of engineered proteins.[16,33] The simplest metal-binding sites are those in which two amino acids with metal-complexing capabilities, mainly histidine residues, are provided by the protein. In the present work sites of this kind, formed by His-X_3-His,[16,33] have been created in solvent-accessible α-helices of the enzyme FNR. The FNR-II mutant was the result of the replacement of lysine residues 290 and 294 by histidines. In the other mutant protein used in the present work only one residue, threonine 119, was replaced by a histidine thus forming the binding site together with the genuine histidine 123 of the native protein. The mildness of the mutation introduced in the α-helices of the enzyme FNR is confirmed by the analysis of the kinetic behavior of the mutants. Table 1 shows that the values of the rate constants, k_{red}, k_2 and k_3, of the two mutants remain basically unchanged as compared with the rate constants calculated for the wild-type enzyme, allowing us to conclude that the introduction of binding sites in the native structure of FNR has not changed the catalytic parameters of the enzyme at all.

It was our aim to investigate if these two structurally identical, but differently located, metal binding sites could orient the binding of the respective FNR on gold surfaces covered with SAMs of thiol terminated with nitrilotriacetic groups, which form tetravalent chelates with metal cations such as Cu^{2+}. Our results indicate that both FNR mutant proteins bear accessible His-X_3-His sites that interact specifically with the two vacant sites of ANTA-Cu^{2+} ligands. Therefore, the position of the binding motif in the protein mutants should tune the orientation and distance of the redox center of the protein to the electrode surface.

All our experimental results are consistent with the interpretation that the proteins are bound to the substrate only through the two histidine residues introduced in the α-helices. The two mutants bind reversibly and specifically to gold surfaces covered with SAM-TOA-ANTA-Cu^{2+}, as is demonstrated by the fact that, in the absence of either the metal in the monolayer or the binding motif on the protein, no binding was observed. The available crystallographic information predicts that once bound through the histidine metal binding motif, FNR-II would have its longitudinal axis parallel to the substrate, whereas mutant FNR-I would have its axis perpendicular to it. The projected area of the two proteins on the electrode surface differs by a factor of about 1.4, this value being very close to the experimental difference by a factor of 1.7 in the amount of bound protein per unit area measured for the two mutants.

The AFM images indicate a smaller distance between individual single mutant molecules than between double mutant ones. Given that the two different orientations exposed different areas of the protein, it could be possible that the interaction between neighbor protein molecules on the electrode surface was also affected by the mutation position. After immobilization FNR-II must have the positively charged ferredoxin binding site oriented toward the gold surface, while the membrane-binding hydrophobic pocket is exposed to the solution.[10] On the contrary, FNR-I should have both interaction sites exposed when bound to the electrode. This could explain the tendency of FNR-II to align in equally spaced rows favored by the interaction of the hydrophobic regions of two adjacent molecules, whereas in the FNR-I the more complex interactions prevent them from organizing in structures showing long-range order.

We also explored the effect of the oriented immobilization on the kinetic constants of the enzyme reaction. The analysis of the catalytic parameters shown in Table 1 indicates that, within experimental error, the immobilization does not affect the performance of either mutant I or II, and that all the molecules immobilized on the SAM covered gold electrode are active.

Further proof that the position of the histidine residues in the protein affects the orientation of the protein relative to the gold substrate was obtained from the results of experiments in which the redox mediator ferrocene was covalently incorporated into the SAM.[34] The orientation of the mutant FNR-II, with the plane of its isoalloxazine ring perpendicular with respect to the electrode surface, was shown to be appropriate for establishing direct electrical contact between the FAD ring and the ferrocene in the monolayer, since electrocatalytic activity was observed in the presence of the enzyme substrate (NADPH). On the contrary, the mutant FNR-I with an orientation of the ring parallel to the SAM surface, and therefore further away from the attached ferrocene, did not show catalytic activity under the same conditions. However, both electrodes displayed similar catalytic currents with soluble ferrocene, suggesting that the lower specific activity of the immobilized single mutant (Table 1) was compensated by a higher amount of protein per unit area (Table 3). The experimental results reported here confirm what we expected, that the distance between the prosthetic group and the electrode surface depends on the location of the binding motif on the protein surface.

Conclusions

We have shown that the binding strategy presented here achieves the goals sought: the mutations introduced in the protein did not alter its kinetic behavior in solution but they determined its specific orientation on the surface of the electrode. Therefore, a general strategy applicable to a large number of proteins with known tertiary structure has been established. This strategy could find application in the design and building of three-dimensional structures such as redox multienzyme complexes,[35a] in the preparation of micrometer-sized micro-analytical minielectrodes[35b] and also in the preparation of enzyme crystals, as it has been shown that different crystal groups can been obtained by introducing a tag at different positions of a protein envelope.[36]

Acknowledgment. We would like to thank Prof. José L. García-Fierro for XPS analysis, Fernando Martinez for the

(32) Regan, L. *Trends Biochem. Sci.* **1995**, *20*, 280−286.

(33) Kellis, J. T., Jr.; Todd, R. J.; Arnold, F. H. *Biotechnology* **1991**, *9*, 994−995.

(34) Incorporation of ferrocene derivatives onto avidine-biotinilated glucose oxidase multilayers has been reported by: Anicet, N.; Anne, A.; Moiroux, J.; Savéant, J.-M. *J. Am. Chem. Soc.* **1998**, *120*, 7115−7116.

(35) (a) Gillett, S. L. *Nanotechnology* **1996**, *7*, 168−176. (b) Grzbowski, B. A.; Haag, R.; Bowden, N.; Whitesides, G. M. *Anal. Chem.* **1998**, *70*, 4645−4652.

(36) Bischler, N.; Balavoine, F.; Milkereit, P.; Tschochner, H.; Mioskowski, C.; Schultz, P. *Biophys. J.* **1998**, *74*, 1522−1532.

(37) Abagyan, R.; Totrov, M.; Kuznetsov, D. *J. Comput. Chem.* **1994**, *15*, 488−506.

aminoferrocene synthesis, and Drs. Claudio Gutierrez and Christian Stadler for a critical reading of the manuscript. J.M.G. was the recipient of a fellowship from the Comunidad de Madrid. J.F.R. was supported by a grant from the Ministerio de Educación y Cultura. The authors thank the Ramón Areces Foundation for its generous support and the CICYT (grant BI097-0912) and European Commission (BIO4-CT97-2199) for financial support.

Supporting Information Available: Figure S1 depicting the chemical structures of the synthetic intermediates, Figure S2 showing cyclic voltammograms of 1 mM $Fe(CN)_6^{3-}$ and 1 mM $Ru(NH_3)_6^{3+}$ on SAM-TOA electrodes at different steps of derivatization, which demonstrate the incorporation of Cu(II), and Figures S3 and S4 showing the reciprocal plots of experimental currents vs FM_{ox} concentration and secondary plots of the *y*-axis intercepts vs NADPH concentration, used to calculate the rate constants of FNR-II and FNR-I electrodes (PDF). This material is available free of charge via the Internet at http://pubs.acs.org.

JA001365M